

# Observations of the Crab Nebula with the HEGRA system of IACTs in convergent mode using a topological trigger

F. Lucarelli <sup>a,b,\*</sup>, A. Konopelko <sup>a</sup>, F. Aharonian <sup>a</sup>,  
W. Hofmann <sup>a</sup>, A. Kohnle <sup>a</sup>, H. Lampeitl <sup>a</sup>, V. Fonseca <sup>b</sup>

<sup>a</sup>*Max-Planck-Institut für Kernphysik, D-69029 Heidelberg, Germany*

<sup>b</sup>*Facultad de Ciencias Físicas, Universidad Complutense, E-28040 Madrid, Spain*

---

## Abstract

Routine observations of the Crab Nebula for a total of about 250 hrs, performed with the HEGRA stereoscopic system of 5 imaging atmospheric Čerenkov telescopes in the standard operational mode, have proven the energy threshold of the system to be 500 GeV for small zenith angles ( $\theta \leq 20^\circ$ ). A *topological trigger* applied along with the *convergent* observational mode allows to reduce noticeably the energy threshold of the system down to 350 GeV. Here we present the relevant Monte Carlo simulations as well as the analysis results of 15 hrs Crab Nebula data taken in such an observational mode. From the Crab Nebula data, the final energy threshold was found to be 350 GeV. The estimated  $\gamma$ -ray flux from the Crab Nebula above 350 GeV is  $(8.1 \pm 0.1_{stat} \pm 0.2_{syst}) \times 10^{-11}$  ph cm<sup>-2</sup> s<sup>-1</sup>, which is consistent with recent measurements reported by the STACEE, CELESTE, CAT, and Whipple groups.

*PACS:* 95.55.Ka; 95.55.Vj; 96.40.Pq

*Keywords:* Imaging Atmospheric Čerenkov Technique; Very High Energy Gamma Ray Astronomy;

---

## 1 Introduction

Ground-based TeV  $\gamma$ -ray astronomy has effectively exploited imaging atmospheric Čerenkov telescopes (IACT) in the study of  $\gamma$ -ray emission arising from a few well established

---

\* Corresponding author.

E-mail address: lucarel@gae.ucm.es

sources, as well as for a general search amongst large numbers of  $\gamma$ -ray source candidates [1]. Given the rather steep energy spectra measured for discovered  $\gamma$ -ray sources as well as for those predicted as potential candidates, a substantial advancement in the sensitivity of IACT techniques can be reached if considerable lowering of the energy threshold<sup>1</sup> of the instrument is achieved. For such spectra the low energy threshold provides a high  $\gamma$ -ray rate, which gives a high sensitivity of the instrument. Nowadays a number of instruments perform observations at the effective energy threshold as low as 250 GeV [1].

Further reduction of the energy threshold could be achieved by using of *(i)* larger optical reflectors (10-20 m in diameter) to increase the photon collection efficiency for the low energy  $\gamma$ -ray showers; *(ii)* imaging cameras equipped with pixels of a relatively small angular size ( $0.1^\circ - 0.15^\circ$ ), to reduce the background night sky light per pixel; and finally, *(iii)* by operating a number of telescopes simultaneously in the *stereoscopic* observational mode, which allows to reduce the trigger threshold by requiring coincidences in a number of telescopes.

The latter approach was proven by the system of 5 imaging atmospheric Čerenkov telescopes built by the HEGRA (*High Energy Gamma-Ray Astronomy*) collaboration at La Palma, Canary Islands. Even for rather small optical reflectors of 8.5 m<sup>2</sup> for each of the telescopes and relatively modest angular size of the camera pixels of  $0.25^\circ$  the energy threshold of the system is about 500 GeV using the nominal observational mode. The corresponding effective dynamic energy range of the  $\gamma$ -ray observations with the HEGRA system of IACTs extends from 500 GeV up to 20 TeV, as shown by the observations of the well established TeV  $\gamma$ -ray source - the Crab Nebula [2]. The extended HEGRA data sample for the Crab Nebula permitted, thanks to the good energy resolution of the HEGRA system of about 10-20%, measurements of the Crab Nebula spectrum with high accuracy over the entire dynamic energy range.

Lowering the energy threshold of the Čerenkov telescopes is not only motivated by the enhancement of the instrument sensitivity but it is also physically important to extend the spectral studies of the  $\gamma$ -ray emission to lower energies. For example, inverse Compton (IC) modeling of the  $\gamma$ -ray spectrum of the Crab Nebula, taken along with the EGRET detection at GeV energies [3,4], predicts a substantial spectral flattening down to energies of 200-300 GeV, whereas above 1 TeV the spectrum has rather a power-law shape of a spectral index of -2.6. The measurement of such change in the spectrum slope would favor the IC model of  $\gamma$ -ray emission. First evidence for deviation from a straightforward power law was suggested by the WHIPPLE group (see [5,6]) and, subsequently, it was confirmed by other measurements made within that energy range by STACEE [7], CELESTE[8], and CAT [9].

In this paper we discuss a new approach to detect low energy  $\gamma$ -rays with the system of HEGRA IACTs by use of a *topological* system trigger along with the *convergent* observational mode. It allows to reduce considerably the trigger threshold and correspondingly

---

<sup>1</sup> The position of a peak in the differential  $\gamma$ -ray detection rate,  $E$  [TeV], is usually assumed as the effective energy threshold of the instrument.

the energy threshold down to 300-350 GeV. Relevant Monte Carlo simulations (see Section III) and trigger tests (see Section IV) have been done in order to prove the efficiency of such observational technique. Finally, we performed 15 hrs observations of the Crab Nebula using the topological trigger technique with the convergent observational mode. Analysis of these data has shown an excess attributed to  $\gamma$ -ray showers at energies well below 500 GeV (Section V-VI). Assuming the shape of the energy spectrum as measured by HEGRA [2] we estimated the integral flux of  $\gamma$ -rays from the Crab Nebula above 350 GeV (Section VII).

## 2 Trigger modes

For most of its operational time the HEGRA IACT system was running using a *standard two-level* trigger [10]. For that, the system telescopes were triggered *locally* when the signals in at least two photomultipliers (PMTs) exceeded a given trigger threshold of 7-8 ph.e.<sup>2</sup> Moreover, those two PMTs should be neighbors (2NN, two-nextneighbour) amongst the 271 PMTs which form the camera. That permits a reduction of the accidental background triggers, caused by the light of the night sky, by a factor of 48. For the second level trigger a *global* (system) trigger requires at least two telescopes being triggered by the same shower within a given coincidence time window. The telescopes CT2, CT4, CT5, and CT6 are  $\simeq 80$  m apart from the central telescope CT3<sup>3</sup> and the inter-telescope coincidence window is set to 70 ns. Detailed comparisons of the actual hardware event rate with the simulations for different trigger configurations and thresholds are given in [11].

A trigger threshold of 7-8 ph.e. is high enough to suppress accidental triggers due to illumination of the camera pixels by background night sky light. At first, the choice of the trigger is determined by the average amount of night sky light photons hitting the camera PMT (pixel) within a trigger gate, which is of 20-30 ns. This value is equivalent to 1 ph.e. for the HEGRA telescopes. It is set by the size of the optical reflector, the angular size of the camera pixels, and the efficiency of the light detectors (PMTs). Secondly, choice of the trigger threshold depends on the designed trigger logics and finally on the total number of camera pixels included into the trigger zone. For a smaller number of pixels in the trigger zone, a reduced number of accidental coincidences is possible, and consequently lower trigger thresholds can be chosen.

Trigger threshold limits the energy of the atmospheric showers, which should be sufficiently powerful to generate a certain number of Čerenkov photons and trigger the camera. Note that low energy  $\gamma$ -ray-induced atmospheric showers can produce a sufficient amount of Čerenkov light photons only at rather small distances from the shower core ( $r \leq 50$  m). Using only 4-telescope coincidences for the HEGRA system of IACTs, these low energy

---

<sup>2</sup> Hereafter ph.e. stands for photoelectrons.

<sup>3</sup> The first telescope (prototype) built by the HEGRA collaboration and numbered CT1, it is not included in the stereoscopic system.

$\gamma$ -ray showers are concentrated within the geometrical area of the array. In addition, the Čerenkov light images of such showers occur in specific parts of the camera for each of the system telescopes, which are determined by the location of the telescopes within the array. By intention, to detect only low energy  $\gamma$ -ray showers, one can restrict the trigger zone to some specific part of the camera, which is sensitive to these events. A reduction of the trigger zone by a factor of about 7 allows to decrease the value of the trigger threshold down to 4 ph.e. and thus achieve a considerable enhancement in the trigger rate of low energy  $\gamma$ -ray showers. This so-called *topological* trigger mode is effective for detection of low energy  $\gamma$ -rays, whereas the rate of the high energy  $\gamma$ -rays well above the energy threshold of the system, will be drastically reduced due to rather narrow trigger zone.

One could try to operate the HEGRA telescopes in standard trigger mode at the very low trigger threshold of 4 ph.e. However, that would imply a drastic increase in the accidental trigger rate of up to 100 Hz and an increase of up to a 30% in the dead time (against a rate of 15 Hz and 5% dead time for the nominal trigger threshold of 7 ph.e.(see [10])). Moreover, current data acquisition system does not support such rate. It would be possible then, to increase the trigger multiplicity and ask for at least 4 telescopes out of 5 to be triggered, but in this case, as we already mentioned previously and we show below through the Monte Carlo simulations, we do not need to use the whole camera, since only certain parts of the camera will be covered by the images of low energy  $\gamma$ -rays.

In the next sections we discuss in detail the implications of using a *topological* trigger mode.

### 3 Simulations

Based on the HEGRA Monte Carlo simulations, we have estimated the detection rates of cosmic rays and  $\gamma$ -rays, as well as the energy threshold of  $\gamma$ -rays for the HEGRA IACT array using a *topological* trigger mode. For such trigger mode one has to use restricted trigger zones within the camera field of view for each of the system telescopes. These zones are adjusted to the regions of most frequent appearance of the  $\gamma$ -ray images. For instance, the restriction on impact distance from the center of the IACT system at 50 m yields a specific distribution of the  $\gamma$ -ray events in the telescope camera focal plane (see Figure 1). Note that the maximum impact distance for the simulated  $\gamma$ -ray showers was 500 m. As it is seen from Figure 1 all events are localized within an angular area roughly corresponding to 19-37 camera pixels. The location of the trigger zone in the camera field of view differs from one telescope to another and is determined by the geometrical layout of the telescopes in the array. In simulations we have assumed that the optical axes of all system telescopes are parallel, which represents the conventional mode of a telescope tracking. One can see in Figure 1 that the corresponding cluster of the triggered events is shifted by about  $0.6^\circ$  from the camera center, which roughly corresponds to 3 camera pixels.

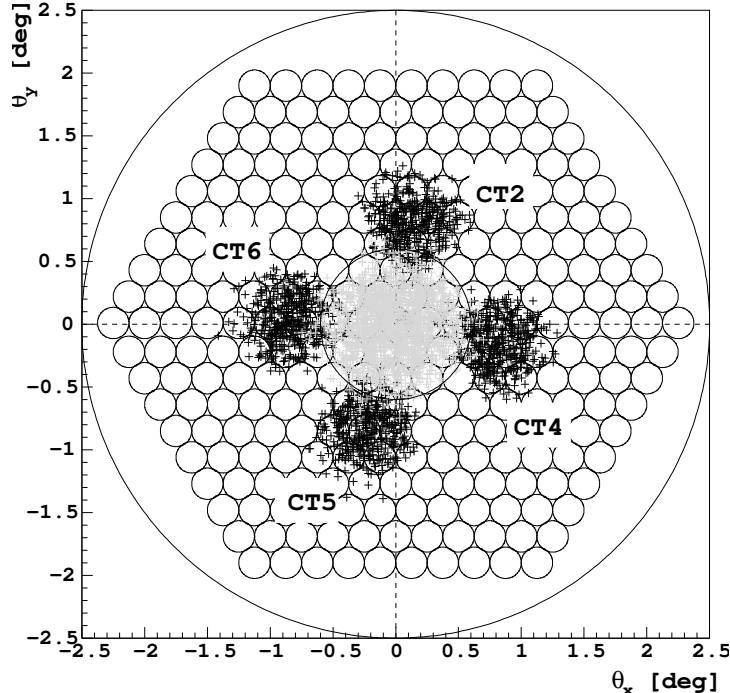


Fig. 1. Two-dimensional distribution of the centroid positions for  $\gamma$ -ray images, triggering at least 4 telescopes of the HEGRA IACT array and passing the selection of the impact distance from the center of the system less than 50 m (black crosses). Simulations have been done for showers at zenith. Data for CT3 are not shown. In convergent mode the centers of gravity are shifted towards the camera center (grey crosses).

We have made calculations of the cosmic and  $\gamma$ -ray detection rates using two different trigger modes: a *standard* local trigger condition of  $2NN/271 > q_0$ , where  $q_0$  is the trigger threshold measured in photoelectrons, and a *topological* trigger mode of  $2NN/19 > q_0$ , where only 19 pixels were selected for each telescope according to the specifically established trigger zone. In both cases, a global trigger mode defined as at least 4 telescopes out of 5 to be triggered by a shower was applied. The detection rates of cosmic rays and  $\gamma$ -rays calculated for different values of trigger thresholds ( $q_0$ ) are shown in Figure 2.

The HEGRA system of IACTs runs in the *standard* trigger mode with the trigger threshold set to  $\simeq 8$  ph.e. That yields a corresponding detection rate of about 4 Hz for the 4-fold coincidences, which is in a good agreement with the measurements. Note that the detection rates of cosmic rays differ by a factor of about 10 between the two different trigger modes (see Figure 2), roughly agreeing with the simple estimate based on the number of the pixels included in the trigger ( $271/19 = 14$ ). In reality, in the experimental data we have found a non uniform rate over the whole camera field of view, which is due to a non equal optical smearing (it is broader at larger angular distances from the center of FoV), restricted number of the trigger patterns for the images being close to the camera edge (i.e., two pixels on the ring), etc. All these effects reduce the number of possible combinations for the  $2NN/M$  trigger logic (which is roughly  $3 \times M$ , where  $M$  is the total number of pixels in the camera, for HEGRA telescopes  $M = 271$ ) and, consequently, the total rate in the standard trigger mode. Using the *topological* trigger mode with the trigger threshold set

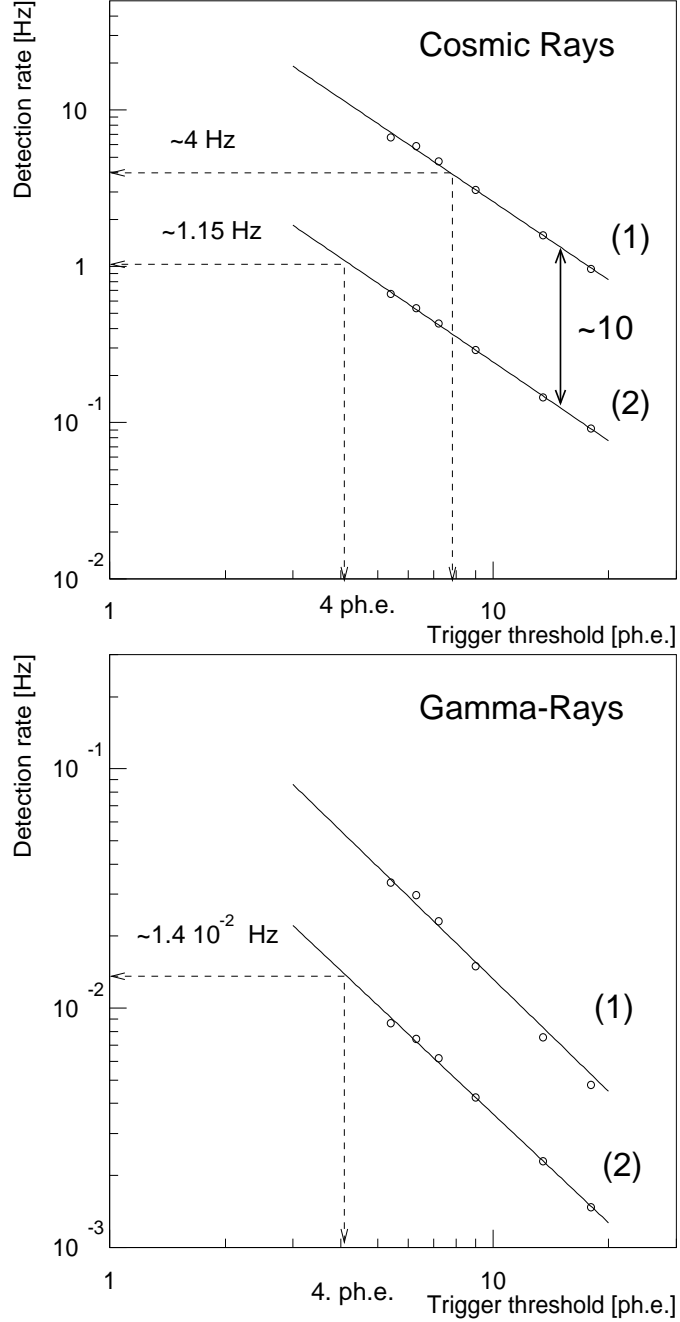


Fig. 2. Detection rates of cosmic rays and  $\gamma$ -rays calculated from MC simulations for different values of trigger thresholds ( $q_0$ ) and for two different trigger modes, (1) standard: 4 telescopes out of 5,  $2NN/271 > q_0$ , and (2) topological: 4 telescopes out of 5,  $2NN/19 > q_0$ . Also the correspondent fits and the rates for  $q_0 = 4$  ph.e. are shown. Simulations have been done for showers at the zenith using parallel tracking in both cases.

at 4 ph.e. the cosmic ray detection rate is about 1.15 Hz. That is somewhat higher than the measured rate for a configuration with 19 pixels in trigger (see section 4). However, given the imperfect adjustment of the trigger window for the rate measurements (due to telescope pointing error) as well as slight differences between Monte Carlo assumed

trigger thresholds and those actually used in observations (e.g. due to a 20% reduced mirror reflectivity etc.), one can conclude that there is a rather good agreement between measured and calculated rates.

For the *topological* trigger mode the calculated  $\gamma$ -ray rate is  $1.4 \cdot 10^{-2}$  Hz (50  $\gamma$ 's per hr) (see Figure 2). In calculations we assumed the  $\gamma$ -ray energy spectrum of the Crab Nebula as measured by the HEGRA collaboration [2]. Dependence of the evaluated energy threshold on the value of the trigger threshold,  $q_0$ [*ph.e.*], can be well fitted by

$$\log(E[\text{TeV}]) = -1.0 + 0.9 \cdot \log(q_0). \quad (1)$$

Thus for the *topological* trigger mode and conventional trigger threshold,  $q_0 = 8$  ph.e., the energy threshold is about 500 GeV, whereas for the reduced trigger threshold,  $q_0 = 4$  ph.e., the energy threshold is of  $\simeq 350$  GeV. Such substantial lowering of the energy threshold by a factor of 1.4 with respect to the *standard* trigger mode could only be achieved by implementing a corresponding upgrade of the telescope hardware, e.g. towards much larger effective collection area of the optical reflector.

For the event classification, both the reconstructed shower direction and the averaged angular size of the Čerenkov light were used in the present analysis. Images recorded at such low energy threshold contain a rather small number of photoelectrons, and image orientation for those events is poorly determined. However, using four images per each individual event one can substantially improve the angular resolution. Thus, for a rather loose angular cut of  $\theta^2 \leq 0.05$  [*deg*<sup>2</sup>], where  $\theta^2$  is the squared angular distance of the reconstructed shower arrival direction to the source position, the Monte Carlo simulations predict a  $\gamma$ -ray acceptance (which is the fraction of remaining events after applying the directional cut),  $\kappa_\gamma^{dir}$ , of about 0.7. The predicted acceptance for the cosmic ray,  $\kappa_{CR}^{dir}$ , is of about 0.05, which corresponds to a rejection factor for the cosmic rays of  $\kappa_{CR}^{-1} \simeq 20$ . Therefore, the directional information results in an enhancement of the signal-to-noise ratio by a factor  $Q^{dir} = \kappa_\gamma^{dir} / \sqrt{\kappa_{CR}^{dir}} \simeq 3.2$ .

Further improvement of the signal-to-noise ratio could be achieved by using the differences in the image shape between the cosmic ray- and  $\gamma$ -ray-induced showers [12]. In general, the angular size of the Čerenkov light images depends on the geometrical distance of the shower axis to the telescope and the primary energy of the shower. For a better separation of the  $\gamma$ -ray images out of the cosmic ray images one has to re-scale the angular image size (WIDTH parameter [12]) with respect to the impact distance and image SIZE (total number of photoelectrons in image) [11]. Showers selected by the *topological* trigger are concentrated within the telescope array, and therefore occur at small impact distances from the center of the array. The dynamic energy range of these events is also very limited, from 100 GeV up to 1 TeV. In such a case the scaling of the angular image size is not necessary, and one can simply use the initial WIDTH parameter for an effective image classification. All triggered cosmic ray and  $\gamma$ -ray events can be plotted versus *mean*

WIDTH  $\langle W \rangle$ , which is calculated as:

$$\langle W \rangle = \frac{\sum_i^N A_i W_i}{\sum_i^N A_i} \quad (2)$$

where  $W_i$  and  $A_i$  are WIDTH parameter and SIZE parameter, respectively, measured for each telescope out of  $N$  ( $N=4$  or  $5$ ) in the system. The mean image SIZE is given by

$$\langle A \rangle = \frac{1}{N} \sum_i^N A_i . \quad (3)$$

Both distributions are shown in Figure 3 for cosmic ray and  $\gamma$ -ray events. One can see in Figure 3 that the parameter  $\langle W \rangle$  enables a rather good rejection of cosmic ray showers. The post-cut  $\gamma$ -ray and cosmic ray acceptances based on the image shape cut are  $\kappa_\gamma^{sh} \simeq 0.72$ ,  $\kappa_{CR}^{sh} \simeq 0.082$ , respectively, with a corresponding signal enhancement factor of  $Q^{sh} = \kappa_\gamma^{sh} / \sqrt{\kappa_{CR}^{sh}} \simeq 2.5$ .

The signal-to-noise ratio in observations with the HEGRA system of IACTs running with the topological trigger for the reduced trigger threshold can be finally estimated as

$$S/N = R_\gamma / (R_{CR})^{1/2} Q^{dir} Q^{sh} \sqrt{t} . \quad (4)$$

For 1 hr observations of the Crab Nebula, we expect a significance  $S/N \simeq 6\sigma$  for a 19

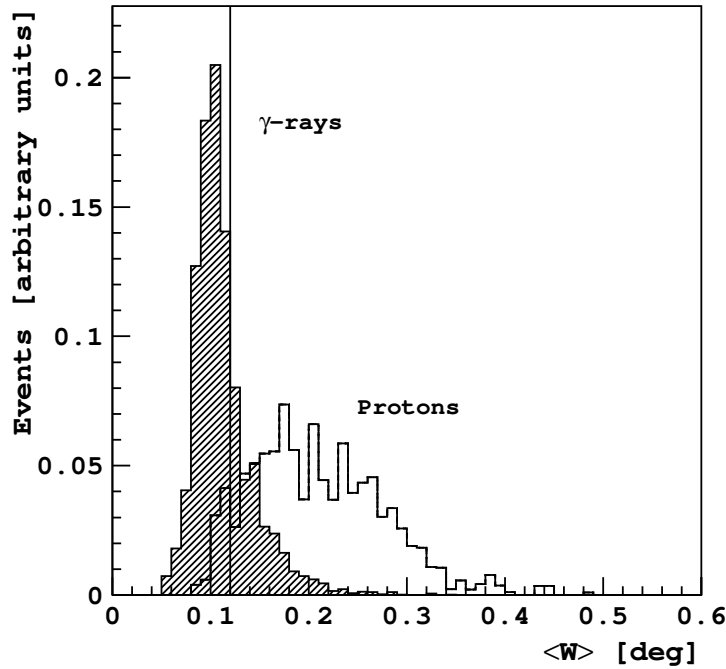


Fig. 3. Distributions of the parameter  $\langle W \rangle$  for cosmic ray and  $\gamma$ -ray showers. The vertical solid line indicates the cut applied in the analysis,  $\langle W \rangle \leq 0.12^\circ$ .



PMT trigger zone. Nevertheless, for the trigger zone of 37 pixels actually used in the observations of the Crab Nebula (see Section V), the integral  $\gamma$ -ray rate from a point-like source remains nearly the same, whereas the rate of cosmic rays, which are randomly distributed over the solid angle, increases due to the substantially broader trigger region. The choice of a 37 pixel trigger zone was forced by the uncertainties in the orientational tilt of the telescopes. Thus we may expect a lower significance of around  $4\sigma/\sqrt{hr}$ . Note that the expected  $\gamma$ -ray rate was calculated assuming the Crab Nebula spectrum at energies above 100 GeV as a power-law with a spectral index of 2.6 and the flux normalization taken from [2]. Actually, as measured by the HEGRA IACTs system [2], the Crab Nebula spectrum shows a slight flattening in the spectrum slope towards low energies, which is consistent with the theoretical expectations (see [3,4]), and which results in a roughly 30% lower  $\gamma$ -ray rate. Thus, the estimate of the trigger performance is finally  $\simeq 3\sigma/\sqrt{hr}$  for a trigger zone of 37 pixels. Therefore, 9 hrs observations (37 pixels trigger mode) will provide a detection of the Crab Nebula above  $\simeq 350$  GeV with a confidence level of  $\sim 9\sigma$ .

#### 4 Tests of the trigger threshold

Trigger configurations for the lowest possible threshold in the *topological* trigger mode as well as the stability for alternating ON and OFF viewing modes<sup>4</sup> were tested in detail for the HEGRA system of IACTs. The trigger threshold was lowered both by decreasing the threshold of the Discriminator-Monitor-Cards (DMC), which are used to verify whether a signal in a single PMT exceeds a certain limit in ph.e. (with a threshold up to 80 mV equivalent to a range of roughly 0 to 70 ph.e.) and generate a 17 ns pulse supplied into the majority unit for the camera (see for detailed discussion [10]), as well as by increasing the high voltage (HV) of the PMTs. 19 pixels were included into the trigger for each camera. The localization of those 19 pixels were calculated using the altitude and azimuth of the viewing angle and the actual position of the telescopes in the array. The system was running in 4-fold coincidence mode. Data runs were taken at 20 degrees of zenith angle. Table 1 gives a summary of the tested configurations. Listed are the gains of the PMTs with respect to the nominal gain  $G_o$ , which is calculated from the mean anode currents in PMTs. The DMC threshold  $q_o^{DMC}$  is given in mV, whereas the threshold  $q_o$  is measured in photoelectrons<sup>5</sup>. The typical system event rate, event rate for individual telescope, and the single pixel rate are summarized in Table 1.  $G/G_0$  ratio indicates the change of the gain after decreasing the threshold, where  $G_0$  is a nominal gain.

The lowest stable trigger threshold before the single pixel rates exploded was found to be 4.0 photoelectrons, which corresponds to a PMT gain of 1.45 times the nominal and the

<sup>4</sup> In the ON and OFF viewing mode, the data are taken while tracking alternatively the source position (ON) and the sky region chosen for estimate of the background (OFF), which is usually placed at  $\pm 5^\circ$  away in right ascension from the nominal source position.

<sup>5</sup>  $q_o^{DMC}$  corresponds to the actual setting of the threshold for the DMC, while  $q_o$  is the value of the threshold converted from mV to ph.e..

Table 1

Summary of the test runs taken with the HEGRA system of IACTs in the topological trigger mode.

$G/G_0$	$q_o^{DMC}$ [mV]	$q_o$ [phe]	System rate [Hz]	Telescope rate [Hz]	Pixel rate [Hz]
1.0	8	6.7	0.41	1-7	$3 \cdot 10^2$
1.53	8	4.38	0.64	5-92	$2 \cdot 10^3$
<b>1.45</b>	<b>7</b>	<b>4.04</b>	<b>0.89</b>	<b>8-320</b>	<b><math>4 \cdot 10^3</math></b>
1.43	6	3.51	0.94	$37-1.8 \cdot 10^3$	$10^4$
2.07	8	3.24	0.19	$2.2 \cdot 10^2 - 7.7 \cdot 10^3$	$1.5 \cdot 10^4$
1.89	7	3.10	0.02	$1.4 \cdot 10^3 - 8.5 \cdot 10^4$	$3 \cdot 10^4$
2.40	8	2.79	0.00	$15-3.7 \cdot 10^3$	$4 \cdot 10^4$

threshold of 7 mV. The system trigger rate was about 0.89 Hz. The nominal threshold was 6.7 photoelectrons, with a DMC threshold of 8 mV, and 1.2 mV/ph.e.. The stability of this configuration was tested by changing night sky background conditions, using a number of 10-minute runs taken with the telescopes positioned at the altitude of  $80^\circ$  and azimuth  $0^\circ$  and brought back to this position at the end of every run. Within given statistics, for different nights and different night sky backgrounds, the system trigger rate was always the same for all of such runs<sup>6</sup>.

## 5 Summary of Crab Nebula data

The observations of the Crab Nebula using the *topological* trigger were performed in the so called *convergent* data taking mode (see [13]) instead of the usual parallel mode. In the convergent observational mode, the optical axes of the telescopes intersect at the typical height of the shower maximum (6-8 km above the sea), instead of being parallel as they are in the standard parallel mode. The *intersection area* in the atmosphere, which is called the active area (see Figure 4), is substantially larger in the case of convergent mode. The convergent mode observations permit to have on average more triggered telescopes per event for the recorded data than the parallel mode. Moreover, in the convergent mode, the centers of gravity of the images in the peripheral telescopes are shifted towards the camera center. That gives significantly fewer events with truncated images at the edge of the camera and permits an easier selection of the trigger active areas (see Figure 1).

<sup>6</sup> Note that, if a PMT current is relatively high due to a presence of a bright star in the field of view, this PMT was automatically switched off.

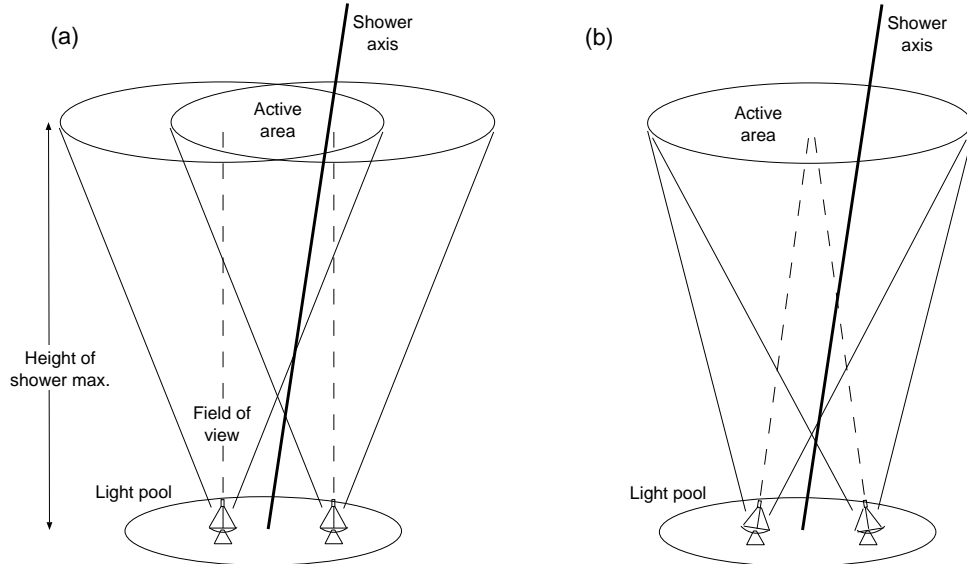


Fig. 4. Schematic view of the parallel (a) and convergent (b) modes for two telescopes. In the convergent observation mode the optical axes of the telescopes intersect at the height of the shower maximum.

The Crab Nebula was observed with the topological trigger mode as described above for a total of 8.7 hours in ON viewing mode and for about 6.1 in OFF viewing mode. Finally, an area of 37 central camera pixels was selected for each telescope, with the trigger condition of 2NN/37. The use of 37 pixels instead of the optimal 19 pixels was motivated by the uncertainty in the tilting angle of system telescopes in the convergent mode. Even a small displacement of a narrow trigger zone composed of 19 pixels with respect to the anticipated angular area of the  $\gamma$ -rays images for a certain tilting angle of 0.6 degree, will lead to a drastic drop of the  $\gamma$ -ray rate. However it is less important for a rather broad trigger zone of 37 pixels. Table 2 summarizes the data and the corresponding rates.

Table 2

Summary of the Crab Nebula data taken with the HEGRA system of IACTs in the topological trigger mode.

Mode:	No. of runs	$T_{OBS}$ [hrs]	Z.A.	System rate [Hz]
ON	27	8.7	$6^\circ \div 30^\circ$	$\sim 1.5$
OFF	20	6.1	$6^\circ \div 30^\circ$	$\sim 1.5$

## 6 Data analysis

A number of checks have been performed in order to verify the  $\gamma$ -ray signal from the Crab Nebula observed with the HEGRA system of IACTs using the topological trigger mode. First, to demonstrate the advancement of the trigger, we have compared the distributions

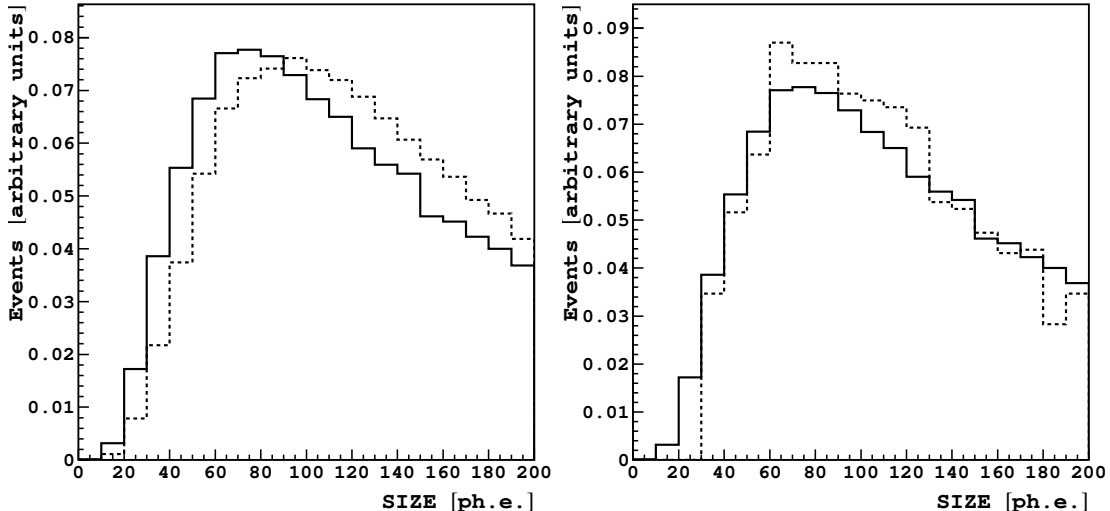


Fig. 5. Left Panel: *Distribution of the SIZE parameter for data taken using the topological trigger (solid line) and normal mode (dashed line).* Right Panel: *Distribution of the SIZE parameter from data (solid line) and MC simulations (dashed line).*

of the measured image SIZE parameter for the standard data taking mode and the topological trigger mode. We also compared the SIZE parameter distributions for data and Monte Carlo events (see Figure 5). The left plot shows that the content of low energy events is more prominent for the topological trigger. In addition, the right panel in Figure 5 shows a good agreement in the SIZE distributions between the data and the Monte Carlo simulations.

Figure 6 shows the distribution of parameter  $\langle W \rangle$  for all recorded excess events, after applying the directional cut of  $\theta^2 < 0.05 [deg^2]$ . The distribution of excess events peaks at  $\langle W \rangle = 0.12^\circ$  and can reproduce well the distribution for the  $\gamma$ -rays derived from the Monte Carlo simulations (see for comparison Figure 3).

Table 3 summarizes the event statistics after applying the directional and shape cuts. The cut on WIDTH parameter  $\langle W \rangle < 0.12^\circ$  corresponds to the optimal cut as predicted by the Monte Carlo simulations. Note that the signal-to-noise ratio (S/N) given in Table 3 was calculated by using the formula of Eqn.(17) from [14], which takes into account a difference in exposure times for ON and OFF, whereas the final estimate of the system signal-to-noise ratio, derived from Monte Carlo simulations (Eqn.(4)), was obtained assuming the same observational time in ON and OFF modes. For the data presented here, the OFF observational time is by factor of 1.4 less than the corresponding time for the ON data

Table 3

Acceptances and corresponding significances after applying the directional and shape cuts to the Crab Nebula data sample taken with the topological trigger mode.

Cuts:	ON	OFF	S/N	S/N/ $\sqrt{hr}$	$\kappa_\gamma$
$\theta^2 < 0.05 [deg^2]; \langle W \rangle < 0.12^\circ$	226	72	6.1	2.1	0.53

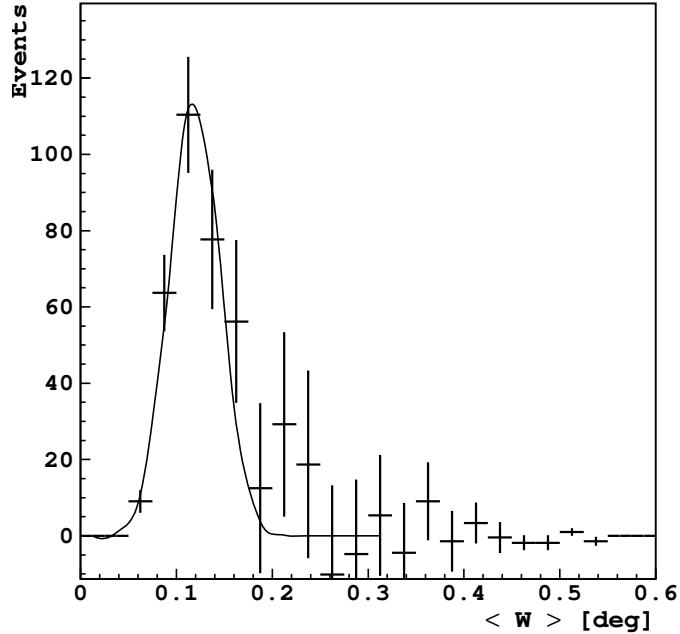


Fig. 6. *Distribution of the excess events over the parameter of weighted WIDTH.*

sample. That explains why the achieved signal-to-noise ratio is slightly lower than one could estimate using Eqn.(4). The  $\gamma$ -ray acceptance,  $\kappa_\gamma$ , reported in Table 3 was calculated from the real data comparing the number of excess events before the angular cut (or a very loose angular cut) with the excess event rate after the actual orientational cut [2].

## 7 Energy threshold and flux estimate

The stereoscopic system permits a straightforward measurement of shower energy, based on the reconstructed impact distance and the measured SIZE of an image (see [11]). For the spectrum studies it is advisable to use a maximal  $\gamma$ -ray acceptance and consequently minimize the systematic error related to the cut efficiency. Here the following cuts were used:  $\langle W \rangle < 0.15^\circ$  and  $\theta^2 < 0.05 [deg^2]$ . The same energy reconstruction routine was used for the Crab Nebula data taken in a standard trigger mode. The distribution of the recorded  $\gamma$ -rays over the reconstructed energy is shown in Figure 7. It is clear that there is a substantial shift of about 40% in the position of the peak, which corresponds to the maximum  $\gamma$ -ray rate. Note that both data samples correspond to similar range of zenith angles. For the topological trigger mode, the position of the peak is between 200-400 GeV. The energy resolution of the HEGRA system of IACTs is  $\Delta E/E \sim 40\%$  at 0.3 TeV,  $\Delta E/E \sim 31\%$  at 0.5 TeV, and  $\Delta E/E \sim 20\%$  at 1 TeV. As it is seen in Figure 7, half of the excess events are below the actual HEGRA energy threshold - 500 GeV. Figure 8 shows, respectively, the distributions of the squared angular distance  $\theta^2$  to the sources (*left panel*) and the WIDTH parameter for those events below the nominal energy threshold (*right panel*).

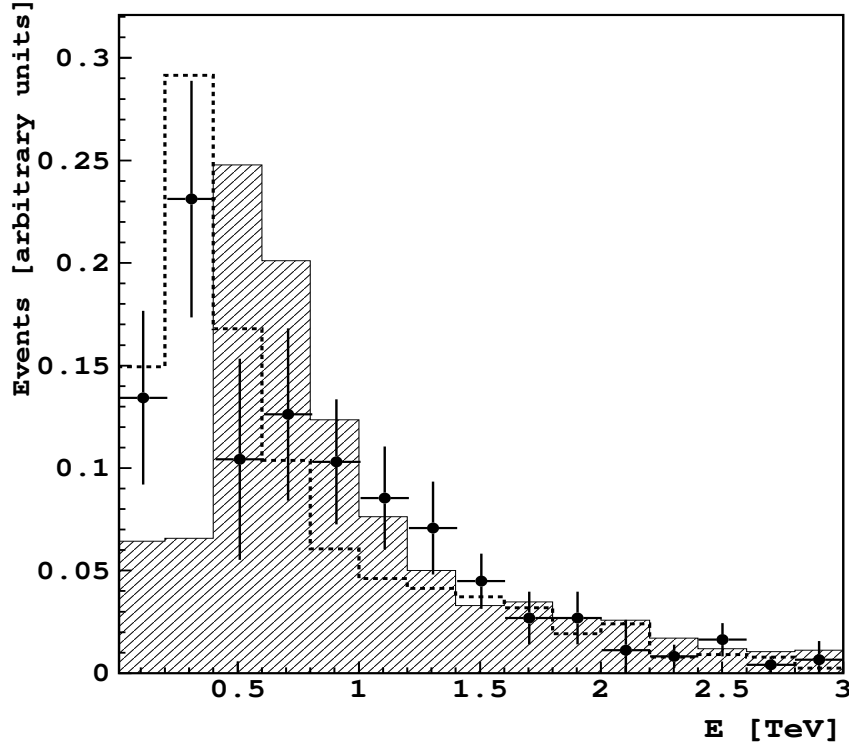


Fig. 7. The energy distribution for the  $\gamma$ -ray events detected from the Crab Nebula, from the data taken in topological trigger mode (black dots) and standard data taking mode (fill hatched histogram). Also superimposed is the MC prediction (dashed line) for the topological trigger mode.

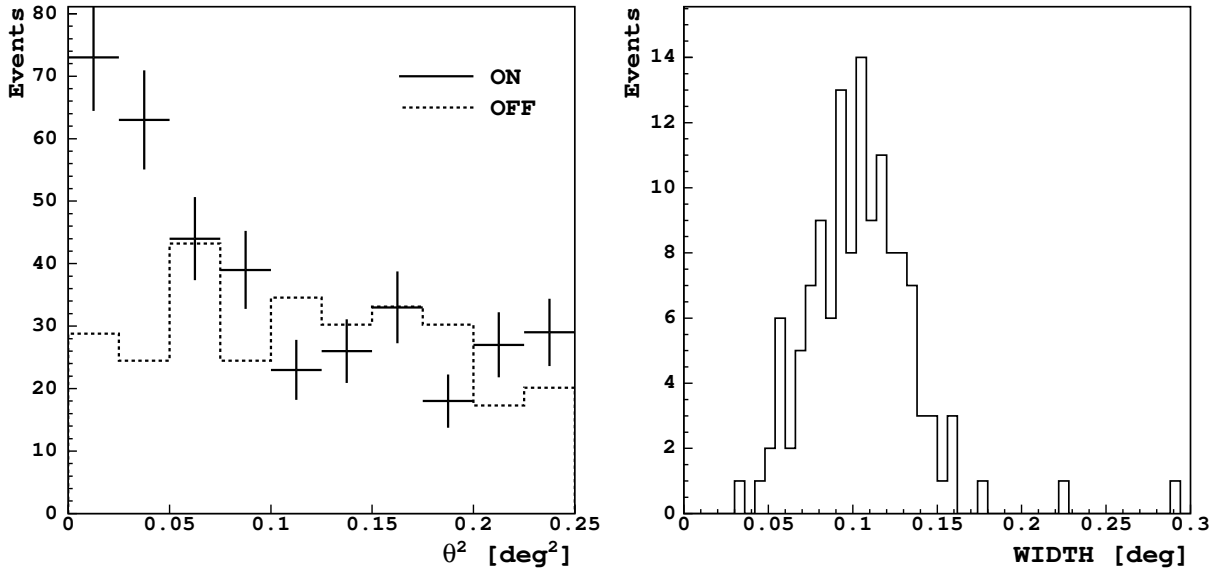


Fig. 8. Left Panel: Squared angular distance  $\theta^2$  of the reconstructed event directions from the Crab direction with reconstructed energies below 500 GeV ( $\langle W \rangle < 0.12^\circ$ ). The OFF data have been scaled by a factor  $T_{\text{ON}}/T_{\text{OFF}} = 1.4$ . Right Panel: WIDTH distribution for CT3 for events with  $E < 500$  GeV.

In estimating the  $\gamma$ -ray flux above the energy threshold, we use the spectral index of the Crab Nebula power law spectrum as measured by the HEGRA system of IACTs above 500 GeV [2], which also takes into account the flattening towards low energies, leaving the normalization factor free:

$$dJ_\gamma/dE = C(E/1 \text{ TeV})^{-2.47-0.11 \log(E)} \text{ ph cm}^{-2}\text{s}^{-1}\text{TeV}^{-1} \quad (5)$$

For such spectrum one can calculate the total number of expected low energy  $\gamma$ -rays

$$\tilde{N}_\gamma = \int_{E_o}^{E_1} (dJ_\gamma/dE) S_\gamma(E) k_\gamma(E) dE \quad (6)$$

where  $S_\gamma$  and  $k_\gamma$  are the collection area and acceptance after the cuts for the  $\gamma$ -rays, respectively.

The boundaries of the integrating regions were selected as  $E_o = 0 \text{ TeV}$  and  $E_1 = \infty$ . By comparing the actual number of recorded  $\gamma$ -ray events,  $N_\gamma$ , with the expected number,  $\tilde{N}_\gamma$ , one can estimate the integral  $\gamma$ -ray flux as

$$J_\gamma(> E_{th}) = (N_\gamma/\tilde{N}_\gamma) \int_{E_{th}}^{E_1} (dJ_\gamma/dE) dE, \quad E_{th} = 350 \text{ GeV} \quad (7)$$

For the loose analysis cuts the total number of registered  $\gamma$ -ray events is  $N_\gamma=260$ , thus the estimated  $\gamma$ -ray flux from the Crab Nebula is

$$J_\gamma(> 350 \text{ GeV}) = (8.1 \pm 0.1 \pm 0.2) \times 10^{-11} \text{ ph cm}^{-2}\text{s}^{-1} \quad (8)$$

Here the estimated statistical and systematic errors are also given. The relative variation  $\Delta J/J$  of the integral flux due to the possible change of the spectral index is of about 6%, while the relative error on the energy estimation is 15%. The estimate of the integral  $\gamma$ -ray flux above 350 GeV derived here is consistent with the measurements by STACEE, CELESTE, WHIPPLE, and CAT groups (see Figure 9). As it is shown in Figure 9, this estimate of the integral  $\gamma$ -ray flux is also consistent with the Inverse Compton model of the TeV  $\gamma$ -ray emission.

## 8 Conclusions

We performed observations of the Crab Nebula with the HEGRA system of IACTs using the *topological trigger mode*, and demonstrated for the first time that it is possible to lower the actual energy threshold of the system by a factor of 1.4 without major hardware changes and, at the same time, keeping the event rate at a sustainable level for

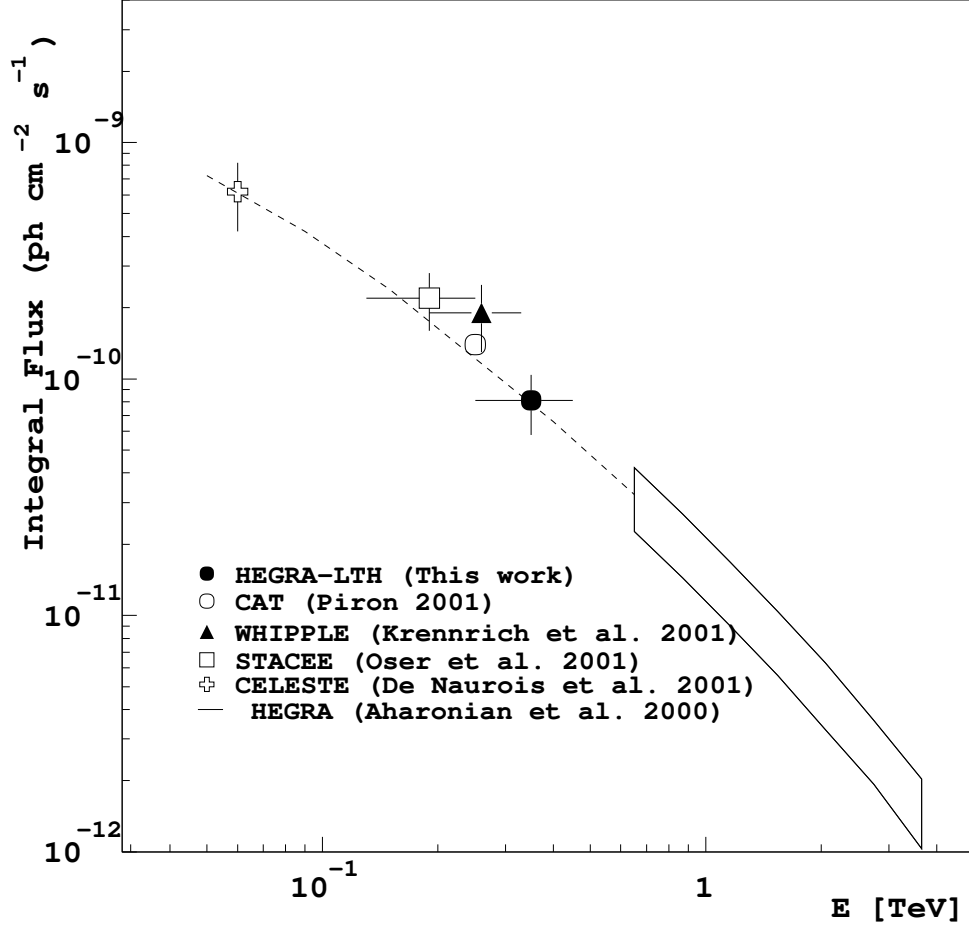


Fig. 9. The integral flux of the  $\gamma$ -rays from the Crab Nebula measured with the HEGRA IACTs array using the topological trigger (black circle). Also shown for comparison are the measurements from other experiments and the upper and lower limits of the systematic error estimated for the HEGRA data. Whipple data were used to calculate the integral flux above 260 GeV by integrating over the spectrum give in [8] and assuming the systematic error of 30%. Dashed curve shows an extrapolation at low energies of the Crab Nebula spectrum as measured by HEGRA which also takes into account a flattening in the spectrum slope towards low energies (see Eq. (5) and [2]).

the currently used DAQ. The Crab Nebula data were taken in fall of 2000 for a total observational time of 15 hrs to check the performance of the system in such observational mode. Here we present the result of the data analysis and give an estimate of the integral  $\gamma$ -ray flux from the Crab Nebula above 350 GeV. Our estimate of the Crab Nebula flux is consistent with previous measurements made by STACEE, CELESTE, and CAT groups, and may be further interpreted as an Inverse Compton TeV emission coming from the plerion in the Crab Nebula.

This technique will be applied in the near future in the observations with the forthcoming H.E.S.S. (*High Energy Stereoscopic System*) system of telescopes, in particular to search for sub TeV  $\gamma$ -ray emission from pulsars [15]. By means of a topological trigger one can achieve a significant reduction of the energy threshold and that gives a considerable advantage in such observations, due to the very steep energy spectrum of the GeV-TeV



pulsed emission as measured by the EGRET detector in the GeV energy range from a number of such objects. It might be also valuable to apply such technique in search for *BL Lac objects at rather large red shifts*, which are expected to have a very steep energy spectrum due to the IR absorption of the  $\gamma$ -rays onto the extragalactic background light.

**Acknowledgments.** The support of the HEGRA experiment by the German Ministry for Research and Technology BMBF and by the Spanish Research Council CICYT is acknowledged. We are grateful to the Instituto de Astrofísica de Canarias for the use of the site and for providing excellent working conditions.

## References

- [1] Catanese, M. and Weekes, T.C. *PASP*, **111**, N **764**, 1193 (1999)
- [2] Aharonian, F., et al. (HEGRA collaboration), *ApJ*, **539**, 317 (2000)
- [3] Atoyan, A. and Aharonian, F., *MNRAS*, **278**, 525 (1996)
- [4] de Jager, O.C., et al., *ApJ*, **457**, 253 (1996)
- [5] Hillas, A.M., et al. (WHIPPLE collaboration), *ApJ*, **503**, 744 (1998)
- [6] Krennrich, F., et al. (WHIPPLE collaboration), *ApJ*, **560**, L45 (2001)
- [7] Oser, S., et al. (STACEE collaboration), *ApJ*, **547**, 949 (2001)
- [8] de Naurois, M., et al. (CELESTE collaboration), *ApJ*, **566**, 343 (2002)
- [9] Piron, F., (CAT collaboration), “*Very high-energy gamma-ray sources as seen by the CAT imaging telescope*”, appeared in Proc. of the 36th Rencontres de Moriond on “Very High-Energy Phenomena in the Universe”, Les Arcs (France), (2001)
- [10] Bulian, N., et al., *Astropart. Phys.*, **8**, **4**, 223 (1998)
- [11] Konopelko, A., et al. (HEGRA collaboration), *Astropart. Phys.*, **4**, 199 (1999)
- [12] Hillas, A.M., *Space Sci. Rev.*, **75**, 17 (1996)
- [13] Lampeitl, H., et al., “*Convergent observations with the stereoscopic HEGRA CT system*”, Poster presented at the TeV Gamma Ray Workshop, Snowbird, (1999) (astro-ph/9910461)
- [14] Li, T., and Ma, Y., *ApJ*, **272**, 317 (1983)
- [15] de Jager, O.C., Konopelko, A., Raubenheimer, B.C. and Visser, B., “*Limits on Pulsar Parameters for Pulsed detections with H.E.S.S*”, appeared in Proc. of the 27th ICRC, Hamburg (Germany), 07-15 August 2001, p. 164 (2001)